HHS Public Access

Author manuscript

*Cell Metab*. Author manuscript; available in PMC 2016 July 07.

Published in final edited form as:

*Cell Metab*. 2015 July 7; 22(1): 175–188. doi:10.1016/j.cmet.2015.05.008.

# Discrete BDNF Neurons in the Paraventricular Hypothalamus Control Feeding and Energy Expenditure

**Juan Ji An**[1], **Guey-Ying Liao**[1], **Clint E. Kinney**[1,2], **Niaz Sahibzada**[2], and **Baoji Xu**[1,*]

[1]Department of Neuroscience, The Scripps Research Institute Florida, Jupiter, FL 33458, USA

[2]Department of Pharmacology and Physiology, Georgetown University Medical Center, Washington, DC 20057, USA

## SUMMARY

Brain-derived neurotrophic factor (BDNF) is a key regulator of energy balance; however, its underlying mechanism remains unknown. By analyzing BDNF-expressing neurons in paraventricular hypothalamus (PVH), we have uncovered neural circuits that control energy balance. The *Bdnf* gene in the PVH was mostly expressed in previously undefined neurons, and its deletion caused hyperphagia, reduced locomotor activity, impaired thermogenesis, and severe obesity. Hyperphagia and reduced locomotor activity were associated with *Bdnf* deletion in anterior PVH, whereas BDNF neurons in medial and posterior PVH drive thermogenesis by projecting to spinal cord and forming polysynaptic connections to brown adipose tissues. Furthermore, BDNF expression in the PVH was increased in response to cold exposure, and its ablation caused atrophy of sympathetic preganglionic neurons. Thus, BDNF neurons in anterior PVH control energy intake and locomotor activity, whereas those in medial and posterior PVH promote thermogenesis by releasing BDNF into spinal cord to boost sympathetic outflow.

## Abstract

[*]Correspondence should be addressed to: bxu@scripps.edu.

**AUTHOR CONTRIBUTIONS**

J.J.A. and B.X. conceived and designed this study, carried out data analysis, and wrote the manuscript. B.X. supervised and coordinated the project. J.J.A. generated mice, carried out behavioral, physiological, imaging, and biochemical experiments. J.J.A., G.Y.L. N.S. and C.E.K. carried out stereotaxic injection. All authors were involved in editing the manuscript.

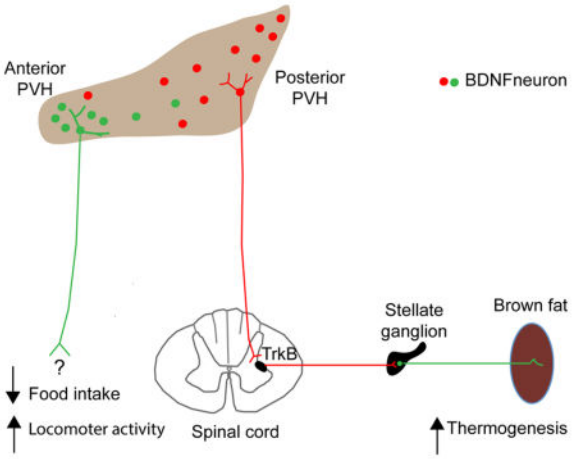


## INTRODUCTION

Changes in body weight result from an imbalance between energy intake and energy expenditure. The central nervous system, especially the hypothalamus, plays a critical role in the control of energy balance (Morton et al., 2006). Several groups of molecularly defined neurons in the hypothalamus have been identified to play a role in regulating energy intake. They include neurons in the arcuate nucleus of the hypothalamus (ARH) that express either agouti-related protein or proopiomelanocortin (Morton et al., 2006); neurons in the paraventricular hypothalamus (PVH) that express the melanocortin-4 receptor (MC4R) (Balthasar et al., 2005); and PVH neurons that express oxytocin (Atasoy et al., 2012). However, delineation of the neural circuitry controlling energy intake is still incomplete, and it remains largely unknown how the brain controls appetite.

Energy is consumed in many biological processes such as thermoregulation and locomotor activity. Some animals produce heat through β-oxidation of fatty acid in brown adipose tissues (BAT) to maintain body temperature. This thermoregulation is a main component of energy expenditure in mice (Garland et al., 2011). Recent studies using new technologies such as positron emission tomography indicate the presence of a significant amount of metabolically active BAT in humans (Whittle et al., 2013). Trans-neuronal tract tracing studies using pseudorabies virus have identified neurons in three PVH divisions that form polysynaptic connection to interscapular BAT (iBAT) in rats: dorsal medial parvicellular part (PVHmpd), ventral medial parvicellular part (PVHmpv) and posterior part (Cano et al., 2003; Oldfield et al., 2002). Neurons in the PVHmpv receive innervation from GABAergic RIP-Cre neurons in the ARH and project to the nucleus tractus solitarius (NTS). The GABAergic transmission from ARH RIP-Cre neurons to the PVHmpv neurons is required for leptin to increase thermogenesis (Kong et al., 2012). However, the role of the neurons in the PVHmpd and posterior PVH in the control of thermogenesis and body weight remains unknown. In sedentary humans and mice, locomotor activity contributes up to 30–40% of daily energy expenditure (Garland et al., 2011). To date, the neural circuitry that governs locomotor activity remains to be uncovered.

Brain-derived neurotrophic factor (BDNF) influences neuronal survival and differentiation as well as synapse formation and plasticity (Waterhouse and Xu, 2009). Substantial evidence also implicates BDNF as a crucial molecule in the control of body weight (Vanevski and Xu, 2013). Mutations in the gene for either BDNF or its receptor TrkB lead to severe obesity in mice (Liao et al., 2012; Rios et al., 2001; Xu et al., 2003). BDNF has been associated with human obesity in genome-wide association studies (Frayling et al., 2007). Furthermore, BDNF and TrkB are among a few ligand-receptor pairs, whose signaling deficiencies lead to severe obesity in human individuals (Farooqi et al., 2000; Han et al., 2008; Montague et al., 1997; Yeo et al., 2004).

It is largely unknown how BDNF regulates energy balance. While it is clear that hyperphagia greatly contributes to obesity developed in humans or mice with deficient BDNF signaling (Han et al., 2008; Rios et al., 2001; Xu et al., 2003; Yeo et al., 2004), it is uncertain whether reduced energy expenditure also contributes to the obesity syndrome. Although delivery of recombinant BDNF into the ventricle or the hypothalamus has been reported to increase energy expenditure (Nonomura et al., 2001; Wang et al., 2010), pair feeding was found to correct excessive weight gain in *Bdnf* heterozygous mice (Coppola and Tessarollo, 2004) and mice lacking the long form of *Bdnf* mRNA (Liao et al., 2012). It also remains unknown which neurons produce BDNF and on which neurons BDNF acts to regulate energy balance. The ventromedial hypothalamus (VMH) has many BDNF-expressing neurons (Xu et al., 2003), and food deprivation selectively and drastically reduces the expression of the *Bdnf* gene in this nucleus (Tran et al., 2006; Unger et al., 2007; Xu et al., 2003). This data suggests that the VMH should produce BDNF to regulate energy balance. However, deletion of the *Bdnf* gene in the VMH and dorsomedial hypothalamus (DMH) only leads to modest obesity (Unger et al., 2007), indicating that the role of VMH BDNF in the control of energy balance is limited. Given that mice and humans with deficient TrkB signaling develop severe obesity, elucidation of the mechanism underlying the effect of BDNF on body weight would provide great insights into the regulation of energy balance.

## RESULTS

### Expression of the *Bdnf* Gene in the PVH

We used $Bdnf^{LacZ/+}$ mice, in which β-galactosidase marks BDNF-expressing cells (Liao et al., 2012), to reveal BDNF expression in the PVH. BDNF neurons were detected throughout the rostrocaudal extent of the PVH (Figures 1A–C). In the medial PVH, the majority of BDNF neurons were in the PVHmpd division (Figure 1B), based on their location (Biag et al., 2012). As BDNF neurons in the cerebral cortex are glutamatergic (Gorski et al., 2003), we examined if BDNF neurons in the PVH also are glutamatergic by using $Bdnf^{LacZ/+};Vglut2^{ires\text{-}Cre/+};Ai9/+$ mice. The *Ai9* locus expresses tdTomato once it is recombined by Cre recombinase (Madisen et al., 2010). Therefore, in these mice tdTomato is expressed in cells expressing VGLUT2, which is one of the three vesicular transporters that are specifically expressed in glutamatergic neurons (Vong et al., 2011). We detected significant colocalization of β-galactosidase with tdTomato in these mice (Figure S1A). This result indicates that many, if not all, BDNF neurons in the PVH are excitatory.

The PVH is a heterogeneous brain structure with many different cell types (Biag et al., 2012). We employed double fluorescence immunohistochemistry on *Bdnf*$^{LacZ/+}$ brain sections to determine whether BDNF neurons belong to some of these molecularly defined neuronal populations. We found that in the PVH there were some coexpression between BDNF and tyrosine hydroxylase (Figures 1D and S1B; 13% of BDNF neurons and 33% of tyrosine hydroxylase neurons) and between BDNF and thyrotropin-releasing hormone (TRH; Figures 1E and S1C; 16% of BDNF neurons and 28% of TRH neurons). However, very few BDNF neurons in the PVH expressed oxytocin (Figure 1F), somatostatin (Figure 1G), growth hormone releasing hormone (GHRH; Figure 1H), corticotropin-releasing hormone (CRH; Figure 1I), or vasopressin (Figure 1J). As MC4R in the PVH has been implicated in the control of energy intake (Balthasar et al., 2005), we also examined coexpression of BDNF with MC4R using the BAC *Mc4r-tau-GFP* mouse strain (Liu et al., 2003). We did not detect coexpression of BDNF and MC4R in the PVH of *Bdnf*$^{LacZ/+}$*;Mc4r-tau-GFP* mice (Figure 1K). Thus, the majority of BDNF neurons likely represent a distinct subset of PVH neurons.

To determine if BDNF expressed in the PVH (PVH BDNF hereafter) may modulate neuronal function in an autocrine fashion, we examined the expression of TrkB in the PVH using *Bdnf*$^{LacZ/+}$*;TrkB*$^{CreERT2/+}$*;Ai9/+* mice. These animals express β-galactosidase in BDNF neurons and tdTomato in TrkB neurons following tamoxifen treatment to induce nuclear localization of the CreERT2 protein. We detected low colocalization of β-galactosidase with tdTomato (Figure 1L; 9% of BDNF neurons and 5% of TrkB neurons), indicating that BDNF and TrkB are largely expressed in distinct cells. Thus, PVH BDNF mainly acts on the nervous system in an anterograde, paracrine, or retrograde manner.

## Obesity in Mice Lacking BDNF Expression in Sim1-Cre Neurons

We tested whether the BAC *Sim1-Cre* transgene, which is highly expressed in the PVH (Balthasar et al., 2005), was suitable to abolish *Bdnf* gene expression in the PVH. *Sim1-Cre* mice were crossed to *Bdnf*$^{klox/+}$ mice to generate *Sim1-Cre;Bdnf*$^{klox/+}$ mice, in which β-galactosidase is expressed in otherwise BDNF-expressing neurons once the floxed *Bdnf*$^{klox}$ allele is deleted by Cre-mediated recombination (Gorski et al., 2003; Liao et al., 2012). We detected many cells expressing β-galactosidase in the PVH (Figures 2A and S2A). We also observed β-galactosidase-expressing cells in some other brain regions (Figures S2B–G), but none in the VMH (Figure S2D), NTS (Figure S2H), dorsal motor nucleus (Figure S2H), and spinal cord (Figure S2I). Thus, *Sim1-Cre* can be used to abolish *Bdnf* gene expression in the PVH in a relatively specific manner.

To understand the role of PVH BDNF in the control of energy balance, we generated a *Bdnf* conditional mutant (*Sim1-Cre;Bdnf*$^{lox/lox}$) by crossing *Sim1-Cre* mice to a floxed *Bdnf* mouse strain (Rios et al., 2001). In situ hybridization confirmed that *Bdnf* gene expression was abolished in the PVH of *Sim1-Cre;Bdnf*$^{lox/lox}$ (Figures 2B and 2C). When fed a standard chow, male and female mutant mice at 20 weeks of age were 41% and 76% heavier than their sex-matched *Bdnf*$^{lox/lox}$ littermates, respectively, whereas *Sim1-Cre* and WT (+/+) mice had comparable body weight to *Bdnf*$^{lox/lox}$ mice (Figures 2D and 2E). These mutant mice also displayed greatly enlarged white adipose tissues (Figure 2F) and increased body length

(Figure 2G). Female mutant mice had higher blood glucose levels than control mice at 20 weeks of age (Figure 2H), and they had already developed impaired glucose tolerance at 16 weeks of age when their blood glucose levels were normal (Figure S2J). Both female and male mutants developed hyperinsulinemia and increased the fasting plasma insulin level by 7.4 and 6.4 fold, respectively (Figure S2K). These results indicate that *Sim1-Cre;Bdnf*$^{lox/lox}$ mice develop obesity in association with abnormal glucose metabolism.

## Hyperphagia and Reduced Energy Expenditure in *Sim1-Cre;Bdnf*$^{lox/lox}$ Mice

We first asked whether increased energy intake was a cause for obesity developed in *Sim1-Cre;Bdnf*$^{lox/lox}$ mice. These animals ingested a similar amount of food as *Bdnf*$^{lox/lox}$ mice at 8 weeks of age (Figure 3A). However, at 20 weeks of age, both male and female *Sim1-Cre;Bdnf*$^{lox/lox}$ mice displayed hyperphagia, as evidenced by 35% and 48% increase in daily food intake, respectively, compared to control mice (Figure 3A). Thus, the absence of BDNF in Sim1-Cre cells causes late-onset hyperphagia.

To determine the contribution of reduced energy expenditure to obesity development in *Sim1-Cre;Bdnf*$^{lox/lox}$ mice, we conducted a pair-feeding experiment. The mutant mice were pair-fed to restrict their daily food intake to the level of *Bdnf*$^{lox/lox}$ mice. Each day, *Sim1-Cre;Bdnf*$^{lox/lox}$ mice were provided the amount of food consumed by their *Bdnf*$^{lox/lox}$ littermates on the previous day, starting at 4 weeks of age when *Sim1-Cre;Bdnf*$^{lox/lox}$ mice were not obese. As expected, both male and female *Sim1-Cre;Bdnf*$^{lox/lox}$ mice with free access to food became obese (Figures 3B and 3C). Although pair feeding did reduce the extent of obesity in *Sim1-Cre;Bdnf*$^{lox/lox}$ mice; these animals still gained significantly more weight than *Bdnf*$^{lox/lox}$ mice (Figures 3B and 3C). Hence, a reduction in energy expenditure is in part responsible for the development of obesity in *Sim1-Cre;Bdnf*$^{lox/lox}$ mice. This was further confirmed by direct assessments of energy expenditure. Oxygen consumption ($VO_2$) was markedly reduced in *Sim1-Cre;Bdnf*$^{lox/lox}$ mice when it was expressed either as per body weight (Figures 3D and 3E) or as per animal (Figure 3F). Additionally, locomotor activity during the dark cycle was decreased in *Sim1-Cre;Bdnf*$^{lox/lox}$ mice (Figure 3G), which would contribute to reduced energy expenditure in these mice.

## Severe Obesity in Mice with BDNF Ablation in the Adult PVH

The obesity phenotype in *Sim1-Cre;Bdnf*$^{lox/lox}$ mice might stem from *Bdnf* deletion in non-PVH neurons (Figures S2B–G). To confirm a role for PVH BDNF in the control of energy balance, we stereotaxically injected purified virus, AAV-Cre-GFP or AAV-GFP, into the PVH of 8-week-old female *Bdnf*$^{lox/lox}$ mice bilaterally. Body weight of these animals was monitored weekly for 8 weeks, while their daily food intake was measured during the 4$^{th}$ and 9$^{th}$ weeks of the post-injection period. Subsequently, these animals were killed and their brains were processed for verification of injection sites. Histological examination showed that not only did we consistently target the PVH (Figures 4A and S3E), but also our AAV injections did not cause significant damage or induce any degeneration in the nucleus (Figures S3A–D). The AAV-Cre-GFP infection abolished BDNF expression in the PVH (Figures 4B and 4C). The animals injected with AAV-Cre-GFP developed obesity, compared to the animals injected with AAV-GFP (Figures 4D and S3F). The obesity phenotype was not due to AAV-Cre-GFP leakage into the anterior hypothalamus and DMH,

as there was no correlation between body weight and the extent of AAV infection in these two hypothalamic areas (Figure S3G). These observations confirm the importance of PVH BDNF to the control of energy balance.

We found that the mice injected with AAV-Cre-GFP could be divided into two groups: AAV-Cre-GFP (MP) group, where GFP was detected in the medial and posterior PVH but little or none in the anterior PVH, and AAV-Cre-GFP (AMP) group, where GFP was detected in the anterior, medial, and posterior PVH (Figure S3G). The AAV-Cre-GFP (AMP) group developed much more severe obesity than the AAV-Cre-GFP (MP) group (Figure 4E). On average, the AAV-Cre-GFP (MP) mice and the AAV-Cre-GFP (AMP) mice consumed 23% and 82% more food than AAV-GFP mice, respectively, during the 4$^{th}$ week of the post-injection period (Figure 4F). The magnitude of hyperphagia in these two groups of mice remained unchanged when food intake was measured again 5 weeks later (Figure S3H), and it was strongly correlated with the extent of AAV-Cre-GFP infection in the anterior PVH (Figure 4G). Thus, BDNF expressed in the anterior PVH is crucial for the control of energy intake.

When normalized to body weight, $VO_2$ was drastically lower in the AAV-Cre-GFP (AMP) mice than control mice at 9 weeks post injection (Figure S3I). When normalized to lean mass, $VO_2$ of the mutant mice was 9% lower than the control mice during the dark cycle, and the difference is close to be significant (Figure S3J, $P$=0.059). Considering that the large amount of adipose tissues in the mutant mice are metabolically less active than other tissues but not inactive and that the mutant mice need energy to ingest and digest extra food, it is likely that $VO_2$ underestimates when normalized to body weight, but overestimates when normalized to lean mass, the energy expenditure of the mutant mice. Therefore, our $O_2$ consumption measurements indicate that *Bdnf* deletion in the adult PVH decreases energy expenditure at least during the dark cycle. In support of this argument, mice in the AAV-Cre-GFP (AMP) group had significantly lower locomotor activity, compared to mice in either the AAV-GFP group or the AAV-Cre-GFP (MP) group (Figure 4H). There was a good correlation between the extent of AAV-Cre-GFP infection in the anterior PVH and reduction in locomotor activity during dark cycle (Figure S3L), but not during light cycle (Figure S3K). These results indicate that BDNF neurons in the anterior PVH are also crucial for the control of locomotor activity.

## Impaired BAT Thermogenesis in Mice Lacking PVH BDNF

We next investigated whether decreased thermogenesis also contributes to reduced energy expenditure in *Sim1-Cre;Bdnf$^{lox/lox}$* mice by analyzing iBAT, the major mediator of thermogenesis (Cannon and Nedergaard, 2004). In 8-week-old *Sim1-Cre;Bdnf$^{lox/lox}$* mice, iBAT was markedly enlarged and pale, compared with that of *Bdnf$^{lox/lox}$* mice (Figures 5A and 5B). Cross section examination of the iBAT showed that the change in size and color was due to lipid accumulation, as *Sim1-Cre;Bdnf$^{lox/lox}$* iBAT contained many cells with a large unilocular lipid droplet, rather than several small lipid droplets found in normal brown adipocytes (Figure 5D). Real-time PCR analysis revealed that levels of mRNA for thermogenic and lipolytic proteins such as uncoupling protein 1 (UCP1), uncoupling protein 3 (UCP3), peroxisome proliferator activated receptor gamma coactivator 1 alpha (PGC1α),

and lipoprotein lipase (Lpl) were drastically reduced, whereas mRNA levels for fatty acid synthase (FAS) was markedly increased in the iBAT of *Sim1-Cre;Bdnf*$^{lox/lox}$ mice (Figure 5C). In contrast, we did not detect significant changes in the expression of these genes in the iBAT of *Bdnf*$^{klox/klox}$ mice (Figure S4A), which lack dendritic BDNF synthesis and develop hyperphagic obesity (Liao et al., 2012). These results indicate that deletion of the *Bdnf* gene in Sim1-Cre cells causes impairment in thermogenesis in association with reduced lipolysis and increased lipid synthesis in brown adipocytes.

As sympathetic outflow is the main determinant of thermogenic and lipolytic activities (Bachman et al., 2002; Rothwell and Stock, 1984), we examined levels of tyrosine hydroxylase in sympathetic axons innervating iBAT. Tyrosine hydroxylase is the rate-limiting enzyme of the norepinephrine synthesis pathway, and its amount is indicative of sympathetic activity. Immunoblotting and immunohistochemistry analyses showed drastically reduced levels of tyrosine hydroxylase in the iBAT of *Sim1-Cre;Bdnf*$^{lox/lox}$ mice (Figures 5E, 5F, and S4B). In agreement with this observation, *Sim1-Cre;Bdnf*$^{lox/lox}$ mice quickly dropped their core body temperature after exposure to 10°C (Figure 5G). Thus, adaptive thermogenesis in BAT is impaired in *Sim1-Cre;Bdnf*$^{lox/lox}$ mice due to reduced sympathetic activity.

To confirm that impaired thermogenesis in *Sim1-Cre;Bdnf*$^{lox/lox}$ mice is due to *Bdnf* deletion in the PVH, we used AAV-Cre-GFP to selectively delete the *Bdnf* gene in the adult PVH as described earlier. The selective ablation of PVH BDNF nearly abolished UCP1 expression (Figures 5H, S4C, and S4D), increased the level of *Fas* mRNA (Figure 5H), and reduced levels of norepinephrine and tyrosine hydroxylase (Figures 5I–K) in the iBAT. Similar to *Sim1-Cre;Bdnf*$^{lox/lox}$ mice, *Bdnf*$^{lox/lox}$ mice receiving AAV-Cre-GFP dropped their core body temperature faster than those receiving AAV-GFP after exposure to 10°C (Figure 5L). Taken together, these results indicate that PVH BDNF stimulates adaptive thermogenesis in iBAT by increasing sympathetic outflow.

## Normal Thyroid Hormone Production and ARH Neurons in *Sim1-Cre;Bdnf*$^{lox/lox}$ Mice

PVH neurons can control thermogenesis through production of thyroid hormones (Lopez et al., 2010). We tested this possibility by examining the expression of the gene for TRH in the PVH and measuring the concentration of thyroid-stimulating hormone (TSH) and triiodothyronine (T3) in the blood. *Sim1-Cre;Bdnf*$^{lox/lox}$ mice had normal levels of *Trh* mRNA in the PVH (Figure S5A) and normal levels of plasma TSH and T3 (Figure S5B and S5C), indicating that the impaired thermogenesis is not due to abnormal production of thyroid hormones.

It has been well documented that target-derived neurotrophic factors are retrogradely transported to cell bodies to regulate neuronal survival and function in the peripheral nervous system (Zweifel et al., 2005). Since many ARH neurons project to the PVH (Morton et al., 2006) and some of them have been implicated in the regulation of thermogenesis (Elias et al., 1998; Kong et al., 2012), we investigated the possibility that PVH BDNF controls thermogenesis through ARH neurons. We detected normal amounts of mRNA in the ARH for all examined genes (Figures S5D and S5E). Thus, it is unlikely that

PVH BDNF controls adaptive thermogenesis by regulating the expression of these genes in the ARH.

## Polysynaptic Connection from PVH BDNF Neurons to iBAT

We then turned our attention to the possibility that PVH BDNF neurons form polysynaptic connections to iBAT and control thermogenesis through this specific neural circuit. We injected GFP-expressing pseudorabies virus (PRV) into the iBAT of *Bdnf*$^{LacZ/+}$ mice or *TrkB*$^{CreERT2/+}$;*Ai9/+* mice that express tdTomato in TrkB neurons (Madisen et al., 2010). Three days after viral injection, we found that the vast majority of PRV-labeled neurons in the PVH were in the PVHmpd (Figures 6D and S6A) and posterior PVH (Figures 6G) divisions and that only a few in the anterior PVH (Figure 6A). Nearly all PRV-labeled neurons in the PVH expressed β-galactosidase (Figures 6A–I), but not tdTomato (Figures 6J–L). PRV also labeled some neurons in the brainstem and intermediolateral column (IML) of the spinal cord (Figures S6D–F), but none in the DMH and VMH (Figures S6B and S6C). Four days after viral injection, we also detected PRV-labeled hypothalamic neurons in the DMH, lateral hypothalamus (LH) and ARH in addition to the PVH (Figures S6G–I). These results indicate that BDNF, but not TrkB neurons, located mainly in the medial and posterior PVH form polysynaptic connections to iBAT. They also suggest that neurons in the DMH, LH and ARH are linked to iBAT through more synapses than BDNF neurons in the PVH.

PVH neurons that are connected to iBAT have been shown to send axons to either the spinal cord or the NTS (Kong et al., 2012; Zhang et al., 2000). To determine whether BDNF neurons in the PVH send axons to these two sites, we injected the retrograde tracer fluorogold into either the T2 region of the spinal cord or the NTS of *Bdnf*$^{LacZ/+}$ mice. Fluorogold injected into the spinal cord labeled many BDNF neurons in the medial and posterior PVH (Figures 6M–O and S6J–L), whereas fluorogold injected into the NTS labeled some BDNF neurons mainly in the posterior PVH (Figures 6P–R and S6M–O). We detected very few fluorogold-labeled BDNF neurons in the anterior PVH, irrespective of the site of fluorogold injection (Figures S6J and S6M). Thus, the majority of BDNF neurons in the medial and posterior PVH directly project to the spinal cord.

## Regulation of Sympathetic Preganglionic Neurons by PVH BDNF

Since PVH BDNF neurons directly project to the thoracic spinal cord and form polysynaptic connections to iBAT, these neurons may innervate sympathetic preganglionic neurons in the IML that are connected to iBAT through the stellate ganglion. If this is true, sympathetic preganglionic neurons in the thoracic IML could become atrophic in *Sim1-Cre;Bdnf*$^{lox/lox}$ mice and in mice where the *Bdnf* gene is selectively deleted in the PVH using AAV-Cre-GFP, assuming that they expresses TrkB and depend on BDNF for maintenance. To this end, we examined whether sympathetic preganglionic neurons expressed TrkB using *TrkB*$^{LacZ/+}$ mice, where the cell bodies and processes of TrkB-expressing neurons are marked by β-galactosidase (Xu et al., 2000). All sympathetic preganglionic neurons that were marked with an antibody against choline acetyltransferase (ChAT) expressed β-galactosidase (Figures 7A–C). ChAT neurons in the thoracic IML of *Sim1-Cre;Bdnf*$^{lox/lox}$ mice had significantly smaller cell bodies, compared to *Bdnf*$^{lox/lox}$ mice (Figures 7D–F), but their number was normal (data not shown). These neurons also had smaller cell bodies in

mice where the *Bdnf* gene was specifically deleted in the adult PVH than in control mice (Figures 7L and S7A). In contrast, IML ChAT neurons had normal cell body size in $Bdnf^{klox/klox}$ mice (Figure S7B), which lack the dendritically localized long form of *Bdnf* mRNA but still have the somatically localized short form of *Bdnf* mRNA whose translation product can be transported to axonal terminals (Liao et al., 2012). Thus, PVH BDNF neurons send axons to innervate and release BDNF to support TrkB-expressing sympathetic preganglionic neurons in the thoracic spinal cord.

The data described above suggest that the neural circuit comprising PVH BDNF neuron → IML cholinergic neuron → stellate ganglion → iBAT plays a key role in the control of thermogenesis and body weight. However, it is unclear if BDNF has an active role in regulating thermogenesis or if it is simply required for the development or maintenance of this neural circuit. To address this issue, we investigated whether *Bdnf* gene expression in the PVH is altered during adaptive thermogenesis. We housed one group of WT mice at 10°C and another group at room temperature (control, 25°C) for 3 days. As expected, the cold exposure increased the expression of *Ucp1*, *Pgc1a*, and *Lpl* in the iBAT (Figure 7G). Interestingly, the treatment also significantly increased *Bdnf* gene expression in the PVH, but not in the VMH (Figures 7H and 7I). This observation suggests that cold exposure may stimulate thermogenesis in part by increasing *Bdnf* gene expression in the PVH.

The observations that IML cholinergic neurons shrink in the absence of PVH BDNF and receive increased BDNF supply from the PVH during adaptation to cold raise the possibility that these neurons are highly plastic and change their size as a mechanism to regulate thermogenesis. Mice decrease adaptive thermogenesis to save energy during food deprivation (Bechtold et al., 2012; Patel et al., 2006). We fasted mice for two days and stained sections of their spinal cords with an antibody against ChAT. In IML cholinergic neurons, the cross area of the cell bodies was reduced by 16%, after a two-day food deprivation (Figures 7J and 7K).

## Requirement of PVH BDNF for Thermogenic Adaption to Food Deprivation

Mice increase adaptive thermogenesis in response to cold exposure (Morrison et al., 2012) or ingestion of high-fat diets (Butler et al., 2001; Kong et al., 2012), while decreasing adaptive thermogenesis in response to food deprivation (Bechtold et al., 2012; Patel et al., 2006). As shown in Figure 5G, PVH BDNF is required for adaptive thermogenesis in response to cold exposure. We measured oxygen consumption in $Bdnf^{lox/lox}$ mice and *Sim1-Cre;*$Bdnf^{lox/lox}$ mice to determine whether high-fat diet ingestion and food deprivation also alter adaptive thermogenesis through BDNF neurons in the PVH.

Ingestion of high-fat diets increases energy expenditure in part by activating thermogenesis. We singly housed 8-week-old $Bdnf^{lox/lox}$ and *Sim1-Cre;*$Bdnf^{lox/lox}$ mice in metabolic cages. Oxygen consumption of these animals was measured for 3 days when fed a low-fat diet (Research Diets D12450B, 10% calories from fat) and for another 3 days when fed a high-fat diet (HFD, Research Diets D12492, 60% calories from fat). *Sim1-Cre;*$Bdnf^{lox/lox}$ mice increased energy expenditure to the same degree as did $Bdnf^{lox/lox}$ mice in response to high-fat diet ingestion (Figure 7M). Thus, PVH BDNF is not essential for adaptive thermogenesis in response to high-fat diet ingestion.

To examine the effect of food deprivation on oxygen consumption, we first allowed 10-week-old *Bdnf*$^{lox/lox}$ and *Sim1-Cre;Bdnf*$^{lox/lox}$ mice to acclimate to metabolic cages for 2 days. Oxygen consumption of these animals was measured for 1 day when the mice had *ad libitum* access to chow and for another 2 days after it was removed. The first-day data served as baseline measurement, while the third-day data reflected the effect of food deprivation. We found that food deprivation reduced $O_2$ consumption in *Bdnf*$^{lox/lox}$ mice, but not in *Sim1-Cre;Bdnf*$^{lox/lox}$ mice (Figure 7N). This result indicates that BDNF neurons in the PVH are involved in the adaptive thermogenesis response to energy deficit.

## DISCUSSION

The hypothalamus is a key brain region in regulating energy intake and body weight, and the output from the PVH mediates much of this hypothalamic control of energy balance (Elmquist et al., 1999). Studies using tissue-specific gene targeting and optogenetic approaches have implicated MC4R neurons and oxytocin neurons of the PVH in the control of energy intake (Atasoy et al., 2012; Balthasar et al., 2005; Shah et al., 2014). We found that BDNF neurons in the PVH expressed neither MC4R nor oxytocin and that ablation of BDNF expression in the PVH led to marked hyperphagia and severe obesity. Thus, our study has uncovered one additional population of PVH neurons that play an important role in regulating energy intake. Given remarkable hyperphagia displayed in mice lacking BDNF expression in the PVH, these BDNF neurons could be more potent in suppressing energy intake than other PVH neuronal groups.

Our results show that PVH BDNF also regulate locomotor activity and BAT thermogenesis. There was a strong correlation of *Bdnf* deletion in the anterior PVH with hyperphagia and reduced locomotor activity, whereas many BDNF neurons in the medial and posterior PVH formed polysynaptic connections to iBAT. Using retrograde tracers and *Bdnf* mutant mice, we were able to delineate a PVH BDNF neuron → sympathetic preganglionic neuron → sympathetic postganglionic neuron → BAT neural circuit, which is distinct from a previously described PVH neural circuit that controls BAT thermogenesis (Kong et al., 2012). Taken together, these observations indicate that discrete groups of BDNF neurons in the PVH control energy intake, locomotor activity, and BAT thermogenesis.

### PVH BDNF and Energy Balance

Mice with mutations in the *Bdnf* gene display marked hyperphagia (Liao et al., 2012; Rios et al., 2001); however, prior to our study neurons that synthesize BDNF to regulate energy intake had not been identified. While food deprivation selectively reduces BDNF expression in the VMH (Tran et al., 2006; Unger et al., 2007; Xu et al., 2003), deletion of the *Bdnf* gene in the VMH using Cre-expressing AAV produces only modest hyperphagic obesity (Unger et al., 2007). We found that deleting the *Bdnf* gene in the PVH using Cre-expressing AAV caused marked hyperphagia and severe obesity. Thus, our study indicates that the PVH is a key brain structure that produces BDNF to control energy intake.

In addition to hyperphagia, deleting the *Bdnf* gene in the PVH also led to low locomotor activity and impaired adaptive BAT thermogenesis, two important components of energy expenditure in mice. This finding appears contradictory to previous observations that show

normal energy expenditure in *Bdnf* heterozygous mice, conditional knockout mice where the *Bdnf* gene is deleted in the DMH and VMH, and mice lacking the long form of *Bdnf* mRNA (Coppola and Tessarollo, 2004; Liao et al., 2012; Unger et al., 2007). *Bdnf* heterozygous mice showed elevated locomotor activity (Kernie et al., 2000), which may compensate for reduced BAT thermogenesis; the conditional knockout mice should still have normal BDNF expression in the PVH to drive BAT thermogenesis and promote locomotor activity; BDNF derived from the short form of *Bdnf* mRNA in the PVH may be sufficient to regulate BAT thermogenesis and locomotor activity. In support of this argument, our data show that young $Bdnf^{klox/klox}$ mice that lack the long form of *Bdnf* mRNA have normal expression of thermogenic genes in iBAT and normal size of IML ChAT neurons. In agreement with our study, administration of BDNF into the ventricle or the hypothalamus has been found to increase energy expenditure (Vanevski and Xu, 2013). Therefore, BDNF also plays key roles in the control of BAT thermogenesis and locomotor activity in addition to regulating energy intake.

We found that mice in which the *Bdnf* gene was deleted in the adult PVH developed much more marked hyperphagia and more severe obesity than *Sim1-Cre;*$Bdnf^{lox/lox}$ mice in which the *Bdnf* gene was deleted in the embryonic PVH. We speculate that this interesting phenomenon is likely due to developmental compensation. Since *TrkB* hypomorphic mutant mice still develop marked hyperphagia and severe obesity even though TrkB expression is down regulated throughout the entire lifespan (Xu et al., 2003), the compensation should occur from up-regulation of BDNF in brain regions outside the PVH, rather than increased activity of other anorexigenic signaling pathways. The same compensation mechanism may explain why deleting the *Bdnf* gene in the adult VMH leads to modest obesity (Unger et al., 2007), whereas deleting the *Bdnf* gene in the embryonic VMH using the *Sf1-Cre* transgene does not alter body weight (Dhillon et al., 2006). These observations suggest that BDNF neurons in some brain structures (including the VMH) other than the PVH also play a role in the regulation of energy balance.

## Role of PVH BDNF Neurons in Energy Intake

MC4R neurons and oxytocin neurons in the PVH have been implicated in the control of energy intake. Deleting the *Mc4r* gene in the PVH using Cre-expressing AAV led to mild hyperphagia and modest obesity (Shah et al., 2014). Suppression of oxytocin neurons in the PVH by GABAergic AgRP neurons produces voracious feeding, but optogenetic activation of the oxytocin neurons does not suppress food intake (Atasoy et al., 2012). In contrast, our study shows that deletion of the *Bdnf* gene in the anterior PVH causes marked hyperphagia and severe obesity. Given that activity stimulates BDNF secretion from neurons (Waterhouse and Xu, 2009), our findings suggest that activation of BDNF neurons in the anterior PVH leads to persistent and powerful suppression of energy intake. Thus, BDNF neurons in the anterior PVH could serve as a key gateway to integrate and relay hypothalamic signals related to adiposity and feeding status to some parts of the CNS to affect energy intake.

BDNF neurons in the PVH are likely to be projection neurons, like those found in other brain regions (Baydyuk et al., 2013; Gorski et al., 2003). Additionally, the vast majority of

these neurons do not express TrkB, and only a fraction of PVH neurons express BDNF or TrkB. Thus, PVH BDNF mainly interacts with TrkB in pre- or post-synaptic neurons to regulate energy intake. We previously reported that BDNF synthesized locally in dendrites is essential for the control of energy intake (Liao et al., 2012). This discovery suggests that TrkB neurons within or outside the PVH innervate dendrites of BDNF neurons in the PVH, and the output of these BDNF neurons suppresses feeding. It will be important to identify neurons that are connected to these BDNF neurons, both pre- and post-synaptically. The presynaptic neurons are likely to be those that sense metabolic signals, while the postsynaptic neurons are likely to affect ingestion behavior.

### Circuit Linking PVH BDNF Neurons to BAT

Some neurons in the PVHmpd, PVHmpv, and posterior PVH are polysynaptically linked to iBAT (Cano et al., 2003; Oldfield et al., 2002). The PVHmpv neurons have been shown to receive innervation from GABAergic RIP-Cre neurons in the ARH and project to the NTS to stimulate thermogenesis (Kong et al., 2012). Our results show that the neurons in the PVHmpd and posterior PVH express BDNF and project to the IML of the spinal cord to stimulate BAT thermogenesis. Because neuronal activity increases BDNF secretion (Waterhouse and Xu, 2009), our observation that deleting the *Bdnf* gene in the PVH impairs adaptive thermogenesis would indicate that activation of BDNF neurons in this nucleus should stimulate thermogenesis. This may explain why administration of glutamate into the PVH produces inconsistent effects on thermogenesis (Morrison et al., 2012), since it would promote thermogenesis through BDNF neurons in the PVMmpd and posterior PVH but inhibit thermogenesis through PVHmpv neurons.

We found that food deprivation reduced the cell body size of sympathetic preganglionic neurons in the spinal cord. This observation suggests that the structure of these neurons is highly plastic and that this structural plasticity could be a mechanism by which adaptive thermogenesis is regulated. BDNF is likely to be a regulator of this plasticity, as our results show that its ablation in the PVH also reduces the size of the cell bodies of these TrkB-expressing neurons. Moreover, cold exposure boosts the BDNF expression in the PVH. It would be interesting to investigate whether dendritic arbors of sympathetic preganglionic neurons are altered in response to food deprivation, cold exposure, and other stimuli that change adaptive thermogenesis.

The ARH RIP-Cre neuron → PVHmpv → NTS circuit and the PVH BDNF neuron → IML circuit may play distinct roles in the control of adaptive thermogenesis. Disruption of the former circuit has been found to impair BAT thermogenesis in response to high-fat diet ingestion (Kong et al., 2012). Our results indicate that the latter circuit is not required for BAT thermogenesis in response to high-fat diet ingestion, although this circuit is essential for adaptive thermogenesis in response to cold exposure. Future studies are needed to address how these two neural circuits interact with each other to regulate adaptive thermogenesis.

# EXPERIMENTAL PROCEDURES

## Animals

*Bdnf*$^{lox/+}$, *Sim1-Cre*, *Mc4r-tau-GFP*, *Ai9*, and *Vglut2-ires-Cre* mouse strains were obtained from the Jackson Laboratory. *Bdnf*$^{LacZ/+}$ and *TrkB*$^{LacZ/+}$ mouse strains were described previously (Liao et al., 2012; Xu et al., 2000). *TrkB*$^{CreERT2/+}$ mice were kindly provided by Dr. David Ginty. *Bdnf*$^{lox/+}$ mice were backcrossed to C57BL/6J mice for at least 10 generations before they were used in this study. Mice were maintained on a 12-h/12-h light/dark cycle with *ad libitum* access to water and a regular rodent chow (LabDiet Mouse Diet 20 with metabolizable energy of 3.56 kcal/g), unless otherwise specified. The Animal Care and Use Committees at Georgetown University and Scripps Florida approved all animal procedures used in this study.

## Physiological Measurements

Measurement of body weight, body length, food intake, fat pads, blood glucose level, and glucose tolerance test were conducted as described previously (Liao et al., 2012). Body composition was determined using a Minispec LF-50/mq 7.5 NMR analyzer (Brucker Optics). Oxygen consumption and locomotor activity were assessed with an indirect calorimeter (TSE System) or a comprehensive lab animal monitoring system (CLAMS, Columbia Instrument). Locomotor activity was measured as light beam breaks in the XY horizontal plane. Fasting serum insulin levels were measured using Ultra Sensitive Mouse Insulin ELISA kit (Crystal Chem).

## In Situ Hybridization, Immunoblotting, and immunohistochemistry

Radioactive in situ hybridization using $^{35}$S-labeled riboprobes and immunoblotting were performed as previously described (An et al., 2008; Xu et al., 2003). Immunohistochemistry was performed as previously described (Liao et al., 2012).

## Stereotaxic Injection of Adeno-Associated Virus

Mice were deeply anesthetized with isoflurane and were placed in a stereotaxic apparatus (David Kopf Instruments). AAV-GFP and AAV-Cre-GFP viruses (serotype 2, UNC vector core) were administered bilaterally into the PVH of 8-week-old female *Bdnf*$^{lox/lox}$ mice using a 10 μl Hamilton syringe with a 33-gauge needle that was attached to a stereotaxic arm. Infusion of each virus (0.15 μl, 1.5 μl/h, $10^{11}$ viral particles/ml) was accomplished by a microsyringe pump (KD Scientific, Holliston, MA) into the PVH region using the following coordinates: anteroposterior, −0.6 mm; mediolateral, +/− 0.35 mm; and dorsoventral, −5.52 mm relative to the bregma. At the end of the infusion, the needle was left in the brain for another 10 min to reduce backflow of the viral injectate along the needle track before it was removed. Following the injection, mice received metacam (1 mg/kg) for analgesia and were returned to their home cages.

## Cold Exposure and Temperature Measurement

Measurement of core body temperature was obtained from mice that were exposed to 10°C for up to 5 hrs by a rectal probe for mice and a thermometer (Thermo Fisher Scientific). The

probe was inserted into the rectum to a depth of 2 cm. All expreiments began at 10 a.m., and the temperature was measured once every hour.

### Pseudorabies Virus Injection

Recombinant pseudorabies virus inoculation was performed in a biosafety level-2 operating room. Two 2.5-μl injections of PRV-152 ($8.5 \times 10^8$ pfu/ml) were made into the brown fat on one side using a Hamilton syringe with a 30-gauge needle.

### Retrograde Neuronal Tracing

*Bdnf*$^{Lacz/+}$ mice were anaesthetized with isoflurane and stereotaxically injected with the retrograde tracer fluorogold (FG, Fluorochrome) into the NTS and thoracic spinal cord. A glass pipette (20–40 μm tip diameter) was used to administer the FG solution (4%, 0.5 μl) into the NTS (coordinates from calamus scriptorius: rostrocaudal, +0.2 mm; mediolateral, 0.1 mm; dorsoventral −0.5 mm) and the thoracic spinal cord at T2 (mediolateral, 0.5 mm; dorsoventral, −0.5mm). One week after microinjection, animals were deeply anesthetized and perfused.

### Statistical analysis

All data are expressed as mean ± SEM. The significance of differences was tested using Student's *t* test, linear regression, or two-way ANOVA with *post-hoc* Bonferroni correction (*, $P < 0.05$; **, $P < 0.01$; and ***, $P < 0.001$).

## Supplementary Material

Refer to Web version on PubMed Central for supplementary material.

## Acknowledgments

We thank D. Ginty for the *TrkB*$^{CreERT2/+}$ mouse strain, L. Enquist for pseudorabies virus, M. Wessendorf for the anti-TRH antibody, and X. Xie for preparation of the graphic abstract. This work was supported by grants from the National Institutes of Health (DK089237 and DK103335) and Klarman Foundation to BX.

## References

An JJ, Gharami K, Liao GY, Woo NH, Lau AG, Vanevski F, Torre ER, Jones KR, Feng Y, Lu B, et al. Distinct role of long 3′ UTR BDNF mRNA in spine morphology and synaptic plasticity in hippocampal neurons. Cell. 2008; 134:175–187. [PubMed: 18614020]

Atasoy D, Betley JN, Su HH, Sternson SM. Deconstruction of a neural circuit for hunger. Nature. 2012; 488:172–177. [PubMed: 22801496]

Bachman ES, Dhillon H, Zhang CY, Cinti S, Bianco AC, Kobilka BK, Lowell BB. betaAR signaling required for diet-induced thermogenesis and obesity resistance. Science. 2002; 297:843–845. [PubMed: 12161655]

Balthasar N, Dalgaard LT, Lee CE, Yu J, Funahashi H, Williams T, Ferreira M, Tang V, McGovern RA, Kenny CD, et al. Divergence of melanocortin pathways in the control of food intake and energy expenditure. Cell. 2005; 123:493–505. [PubMed: 16269339]

Baydyuk M, Xie Y, Tessarollo L, Xu B. Midbrain-derived neurotrophins support survival of immature striatal projection neurons. J Neurosci. 2013; 33:3363–3369. [PubMed: 23426664]

Bechtold DA, Sidibe A, Saer BR, Li J, Hand LE, Ivanova EA, Darras VM, Dam J, Jockers R, Luckman SM, et al. A role for the melatonin-related receptor GPR50 in leptin signaling, adaptive thermogenesis, and torpor. Curr Biol. 2012; 22:70–77. [PubMed: 22197240]

Biag J, Huang Y, Gou L, Hintiryan H, Askarinam A, Hahn JD, Toga AW, Dong HW. Cyto- and chemoarchitecture of the hypothalamic paraventricular nucleus in the C57BL/6J male mouse: a study of immunostaining and multiple fluorescent tract tracing. J Comp Neurol. 2012; 520:6–33. [PubMed: 21674499]

Butler AA, Marks DL, Fan W, Kuhn CM, Bartolome M, Cone RD. Melanocortin-4 receptor is required for acute homeostatic responses to increased dietary fat. Nat Neurosci. 2001; 4:605–611. [PubMed: 11369941]

Cannon B, Nedergaard J. Brown adipose tissue: function and physiological significance. Physiological reviews. 2004; 84:277–359. [PubMed: 14715917]

Cano G, Passerin AM, Schiltz JC, Card JP, Morrison SF, Sved AF. Anatomical substrates for the central control of sympathetic outflow to interscapular adipose tissue during cold exposure. The Journal of comparative neurology. 2003; 460:303–326. [PubMed: 12692852]

Coppola V, Tessarollo L. Control of hyperphagia prevents obesity in BDNF heterozygous mice. Neuroreport. 2004; 15:2665–2668. [PubMed: 15570174]

Dhillon H, Zigman JM, Ye C, Lee CE, McGovern RA, Tang V, Kenny CD, Christiansen LM, White RD, Edelstein EA, et al. Leptin directly activates SF1 neurons in the VMH, and this action by leptin is required for normal body-weight homeostasis. Neuron. 2006; 49:191–203. [PubMed: 16423694]

Elias CF, Lee C, Kelly J, Aschkenasi C, Ahima RS, Couceyro PR, Kuhar MJ, Saper CB, Elmquist JK. Leptin activates hypothalamic CART neurons projecting to the spinal cord. Neuron. 1998; 21:1375–1385. [PubMed: 9883730]

Elmquist JK, Elias CF, Saper CB. From lesions to leptin: hypothalamic control of food intake and body weight. Neuron. 1999; 22:221–232. [PubMed: 10069329]

Farooqi IS, Yeo GS, Keogh JM, Aminian S, Jebb SA, Butler G, Cheetham T, O'Rahilly S. Dominant and recessive inheritance of morbid obesity associated with melanocortin 4 receptor deficiency. J Clin Invest. 2000; 106:271–279. [PubMed: 10903343]

Frayling TM, Timpson NJ, Weedon MN, Zeggini E, Freathy RM, Lindgren CM, Perry JR, Elliott KS, Lango H, Rayner NW, et al. A common variant in the FTO gene is associated with body mass index and predisposes to childhood and adult obesity. Science. 2007; 316:889–894. [PubMed: 17434869]

Garland T Jr, Schutz H, Chappell MA, Keeney BK, Meek TH, Copes LE, Acosta W, Drenowatz C, Maciel RC, van Dijk G, et al. The biological control of voluntary exercise, spontaneous physical activity and daily energy expenditure in relation to obesity: human and rodent perspectives. J Exp Biol. 2011; 214:206–229. [PubMed: 21177942]

Gorski JA, Zeiler SR, Tamowski S, Jones KR. Brain-derived neurotrophic factor is required for the maintenance of cortical dendrites. J Neurosci. 2003; 23:6856–6865. [PubMed: 12890780]

Han JC, Liu QR, Jones M, Levinn RL, Menzie CM, Jefferson-George KS, Adler-Wailes DC, Sanford EL, Lacbawan FL, Uhl GR, et al. Brain-derived neurotrophic factor and obesity in the WAGR syndrome. N Engl J Med. 2008; 359:918–927. [PubMed: 18753648]

Kernie SG, Liebl DJ, Parada LF. BDNF regulates eating behavior and locomotor activity in mice. Embo J. 2000; 19:1290–1300. [PubMed: 10716929]

Kong D, Tong Q, Ye C, Koda S, Fuller PM, Krashes MJ, Vong L, Ray RS, Olson DP, Lowell BB. GABAergic RIP-Cre neurons in the arcuate nucleus selectively regulate energy expenditure. Cell. 2012; 151:645–657. [PubMed: 23101631]

Liao GY, An JJ, Gharami K, Waterhouse EG, Vanevski F, Jones KR, Xu B. Dendritically targeted Bdnf mRNA is essential for energy balance and response to leptin. Nat Med. 2012; 18:564–571. [PubMed: 22426422]

Liu H, Kishi T, Roseberry AG, Cai X, Lee CE, Montez JM, Friedman JM, Elmquist JK. Transgenic mice expressing green fluorescent protein under the control of the melanocortin-4 receptor promoter. J Neurosci. 2003; 23:7143–7154. [PubMed: 12904474]

Lopez M, Varela L, Vazquez MJ, Rodriguez-Cuenca S, Gonzalez CR, Velagapudi VR, Morgan DA, Schoenmakers E, Agassandian K, Lage R, et al. Hypothalamic AMPK and fatty acid metabolism mediate thyroid regulation of energy balance. Nature medicine. 2010; 16:1001–1008.

Madisen L, Zwingman TA, Sunkin SM, Oh SW, Zariwala HA, Gu H, Ng LL, Palmiter RD, Hawrylycz MJ, Jones AR, et al. A robust and high-throughput Cre reporting and characterization system for the whole mouse brain. Nat Neurosci. 2010; 13:133–140. [PubMed: 20023653]

Montague CT, Farooqi IS, Whitehead JP, Soos MA, Rau H, Wareham NJ, Sewter CP, Digby JE, Mohammed SN, Hurst JA, et al. Congenital leptin deficiency is associated with severe early-onset obesity in humans. Nature. 1997; 387:903–908. [PubMed: 9202122]

Morrison SF, Madden CJ, Tupone D. Central control of brown adipose tissue thermogenesis. Front Endocrinol (Lausanne). 2012; 3:5.

Morton GJ, Cummings DE, Baskin DG, Barsh GS, Schwartz MW. Central nervous system control of food intake and body weight. Nature. 2006; 443:289–295. [PubMed: 16988703]

Nonomura T, Tsuchida A, Ono-Kishino M, Nakagawa T, Taiji M, Noguchi H. Brain-derived neurotrophic factor regulates energy expenditure through the central nervous system in obese diabetic mice. Int J Exp Diabetes Res. 2001; 2:201–209. [PubMed: 12369708]

Oldfield BJ, Giles ME, Watson A, Anderson C, Colvill LM, McKinley MJ. The neurochemical characterisation of hypothalamic pathways projecting polysynaptically to brown adipose tissue in the rat. Neuroscience. 2002; 110:515–526. [PubMed: 11906790]

Patel HR, Qi Y, Hawkins EJ, Hileman SM, Elmquist JK, Imai Y, Ahima RS. Neuropeptide Y deficiency attenuates responses to fasting and high-fat diet in obesity-prone mice. Diabetes. 2006; 55:3091–3098. [PubMed: 17065347]

Rios M, Fan G, Fekete C, Kelly J, Bates B, Kuehn R, Lechan RM, Jaenisch R. Conditional deletion of brain-derived neurotrophic factor in the postnatal brain leads to obesity and hyperactivity. Mol Endocrinol. 2001; 15:1748–1757. [PubMed: 11579207]

Rothwell NJ, Stock MJ. Effects of denervating brown adipose tissue on the responses to cold, hyperphagia and noradrenaline treatment in the rat. J Physiol. 1984; 355:457–463. [PubMed: 6491999]

Shah BP, Vong L, Olson DP, Koda S, Krashes MJ, Ye C, Yang Z, Fuller PM, Elmquist JK, Lowell BB. MC4R-expressing glutamatergic neurons in the paraventricular hypothalamus regulate feeding and are synaptically connected to the parabrachial nucleus. Proc Natl Acad Sci U S A. 2014

Tran PV, Akana SF, Malkovska I, Dallman MF, Parada LF, Ingraham HA. Diminished hypothalamic bdnf expression and impaired VMH function are associated with reduced SF-1 gene dosage. J Comp Neurol. 2006; 498:637–648. [PubMed: 16917842]

Unger TJ, Calderon GA, Bradley LC, Sena-Esteves M, Rios M. Selective deletion of Bdnf in the ventromedial and dorsomedial hypothalamus of adult mice results in hyperphagic behavior and obesity. J Neurosci. 2007; 27:14265–14274. [PubMed: 18160634]

Vanevski F, Xu B. Molecular and neural bases underlying roles of BDNF in the control of body weight. Frontiers in neuroscience. 2013; 7:37. [PubMed: 23519010]

Vong L, Ye C, Yang Z, Choi B, Chua S Jr, Lowell BB. Leptin action on GABAergic neurons prevents obesity and reduces inhibitory tone to POMC neurons. Neuron. 2011; 71:142–154. [PubMed: 21745644]

Wang C, Bomberg E, Billington CJ, Levine AS, Kotz CM. Brain-derived neurotrophic factor (BDNF) in the hypothalamic ventromedial nucleus increases energy expenditure. Brain Res. 2010; 1336:66–77. [PubMed: 20398635]

Waterhouse EG, Xu B. New insights into the role of brain-derived neurotrophic factor in synaptic plasticity. Mol Cell Neurosci. 2009; 42:81–89. [PubMed: 19577647]

Whittle A, Relat-Pardo J, Vidal-Puig A. Pharmacological strategies for targeting BAT thermogenesis. Trends in pharmacological sciences. 2013; 34:347–355. [PubMed: 23648356]

Xu B, Goulding EH, Zang K, Cepoi D, Cone RD, Jones KR, Tecott LH, Reichardt LF. Brain-derived neurotrophic factor regulates energy balance downstream of melanocortin-4 receptor. Nat Neurosci. 2003; 6:736–742. [PubMed: 12796784]

Xu B, Zang K, Ruff NL, Zhang YA, McConnell SK, Stryker MP, Reichardt LF. Cortical degeneration in the absence of neurotrophin signaling: dendritic retraction and neuronal loss after removal of the receptor TrkB. Neuron. 2000; 26:233–245. [PubMed: 10798407]

Yeo GS, Connie Hung CC, Rochford J, Keogh J, Gray J, Sivaramakrishnan S, O'Rahilly S, Farooqi IS. A de novo mutation affecting human TrkB associated with severe obesity and developmental delay. Nat Neurosci. 2004; 7:1187–1189. [PubMed: 15494731]

Zhang YH, Lu J, Elmquist JK, Saper CB. Lipopolysaccharide activates specific populations of hypothalamic and brainstem neurons that project to the spinal cord. The Journal of neuroscience: the official journal of the Society for Neuroscience. 2000; 20:6578–6586. [PubMed: 10964963]

Zweifel LS, Kuruvilla R, Ginty DD. Functions and mechanisms of retrograde neurotrophin signalling. Nat Rev Neurosci. 2005; 6:615–625. [PubMed: 16062170]

## HIGHLIGHTS

- The PVH is a key structure that produces BDNF to control energy balance
- The majority of BDNF neurons in the PVH are distinct from previously defined ones
- BDNF neurons in the anterior PVH inhibit feeding and stimulate locomotor activity
- BDNF neurons in the medial and posterior PVH drive adaptive thermogenesis

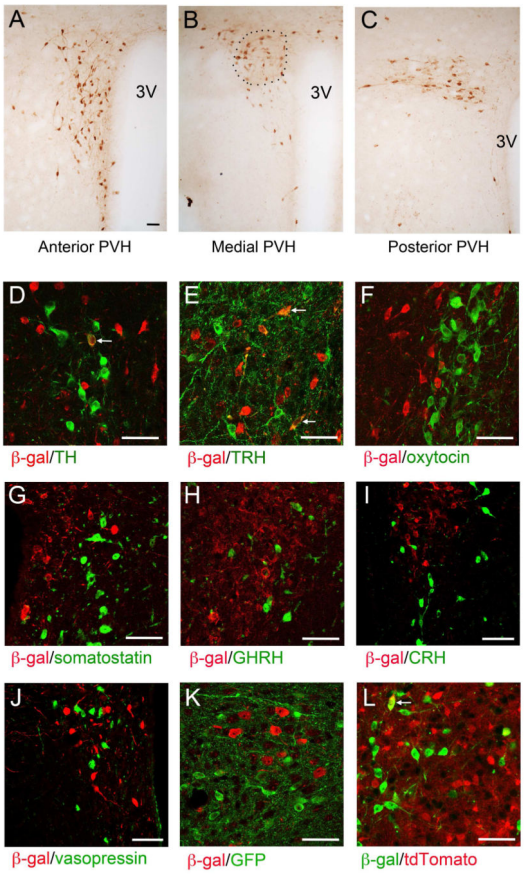


**Figure 1. BDNF expression in the PVH as revealed by anti-β-galactosidase immunohistochemistry in *Bdnf*$^{LacZ/+}$ mice**

(A–C) Immunohistochemistry images showing the distribution of BDNF expression in the PVH. The approximate location of the PVHmpd is outlined. 3V, the 3$^{rd}$ ventricle.

(D–J) Coexpression of BDNF with tyrosine hydroxylase (TH), thyrotropin-releasing hormone (TRH), oxytocin, somatostatin, growth hormone releasing hormone (GHRH), corticotropin-releasing hormone (CRH), and vasopressin in the PVH. BDNF-expressing neurons were marked by β-galactosidase (β-gal) in *Bdnf*$^{LacZ/+}$ mice. Arrows denote representative BDNF neurons that also express TH or TRH.

(K) Coexpression of BDNF with MC4R in the PVH. BDNF- and MC4R-expressing neurons were marked with β-galactosidase and GFP, respectively, in *Bdnf*$^{LacZ/+}$*;Mc4r-tau-GFP* mice.

(L) Coexpression of BDNF with TrkB in the PVH. BDNF- and TrkB-expressing neurons were marked with β-galactosidase and tdTomato, respectively, in *Bdnf*$^{LacZ/+}$*;TrkB*$^{CreERT2/+}$*;Ai9/+* mice. The arrow denotes a representative BDNF neuron that also expresses TrkB.

The scale bar represents 50 μm. See also Figure S1.

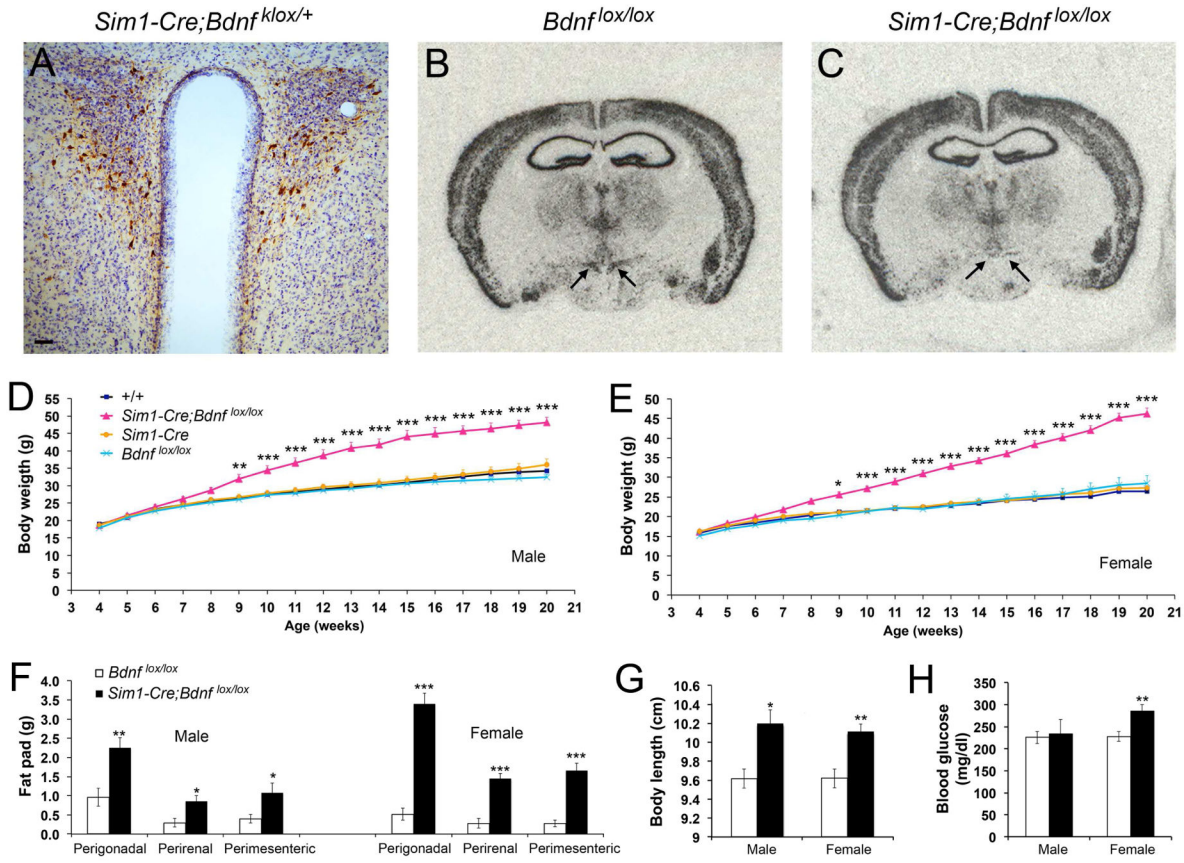


**Figure 2. Deletion of the *Bdnf* gene in the PVH using the *Sim1-Cre* transgene**

(A) Immunohistochemistry image showing β-galactosidase-expressing neurons in the PVH of *Sim1-Cre;Bdnf*$^{klox/+}$ mice. The brain section was counterstained with Nissl. The scale bar represents 50 μm.

(B and C) *In situ* hybridization of *Bdnf* mRNA revealing abolishment of *Bdnf* gene expression in the PVH of *Sim1-Cre;Bdnf*$^{lox/lox}$ mice at 4 months of age. Arrows denote the PVH.

(D) Body weight of male *Sim1-Cre;Bdnf*$^{lox/lox}$ mice and littermate controls. Two-way ANOVA indicates a significant effect of genotypes on body weight: $F_{(3, 663)} = 379.84$ (n=9–14 mice per genotype), $P < 0.001$.

(E) Body weight of female *Sim1-Cre;Bdnf*$^{lox/lox}$ mice and littermate controls. Two-way ANOVA indicates a significant effect of genotypes on body weight: $F_{(3, 612)} = 462.53$ (n=8–13 mice per genotype), $P < 0.001$.

(F – H) Fat pad mass, body length, and blood glucose levels in *Bdnf*$^{lox/lox}$ mice and *Sim1-Cre;Bdnf*$^{lox/lox}$ mice at 20 weeks of age (n=5–8 mice per group).

Error bars indicate standard errors. See also Figure S2.

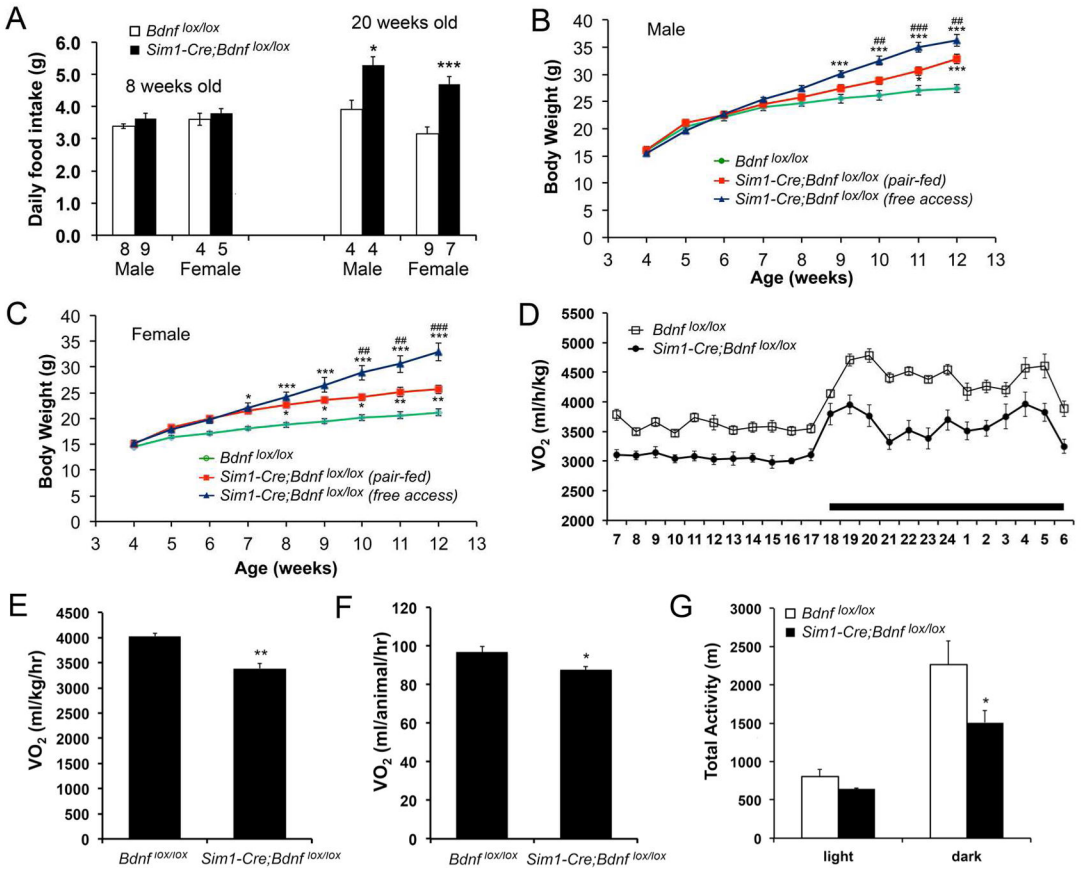


**Figure 3. Reduced energy expenditure in *Sim1-Cre;Bdnf*$^{lox/lox}$ mice**

(A) Daily food intake at 8 and 20 weeks of age. The numbers of mice used are indicated under each column.

(B) Body weight of male *Sim1-Cre;Bdnf*$^{lox/lox}$ mice with free access to food or fed with the amount of food ingested by male *Bdnf*$^{lox/lox}$ mice. Two-way ANOVA for the effect of treatment on body weight: $F_{(2, 198)} = 57.22$ (n=7–10 mice per group), $P < 0.001$. * $P < 0.05$ and *** $P < 0.001$ when compared to *Bdnf*$^{lox/lox}$ mice using Bonferroni post-hoc test. $^{\#\#}$ $P < 0.01$ and $^{\#\#\#}$ $P < 0.001$ when mutant mice with free access to food were compared to pair-fed mutant mice using Bonferroni post-hoc test.

(C) Body weight of female *Sim1-Cre;Bdnf*$^{lox/lox}$ mice with free access to food or fed with the amount of food ingested by female *Bdnf*$^{lox/lox}$ mice. Two-way ANOVA for the effect of treatment on body weight: $F_{(2, 198)} = 102.12$ (n=6–11 mice per group), $P < 0.001$. * $P < 0.05$, ** $P < 0.01$, and *** $P < 0.001$ when compared to *Bdnf*$^{lox/lox}$ mice using Bonferroni post-hoc test. $^{\#\#}$ $P < 0.01$ and $^{\#\#\#}$ $P < 0.001$ when mutant mice with free access to food were compared to pair-fed mutant mice using Bonferroni post-hoc test.

(D) Distribution of $VO_2$ over a 24-hr period in male mice at 8 weeks of age. The body weights of the mice were 24.0 ± 0.5 g for *Bdnf*$^{lox/lox}$ and 26.1 ± 1.3 g for *Sim1-Cre;Bdnf*$^{lox/lox}$ ($P = 0.143$). Two-way ANOVA for the effect of genotype: $F_{(1, 216)} = 359.74$ (n=5–6 per genotype), $P < 0.001$.

(E–G) Oxygen consumption and locomotor activity of male *Bdnf*$^{lox/lox}$ and *Sim1-Cre;Bdnf*$^{lox/lox}$ mice at 8 weeks of age (n=5–6 mice per genotype).

Error bars indicate standard errors.

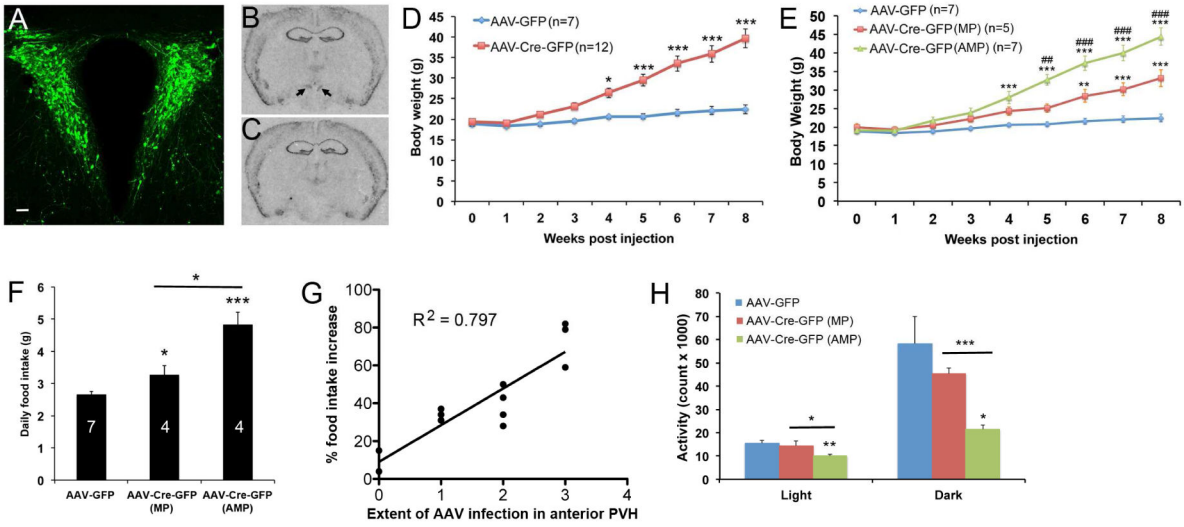


**Figure 4. Deletion of the *Bdnf* gene in the adult PVH using Cre-expressing AAV**

(A) Injection of AAV-GFP into the PVH. The scale bar represents 50 μm.

(B and C) *In situ* hybridization of *Bdnf* mRNA in brain sections of $Bdnf^{lox/lox}$ mice injected with either AAV-GFP (B) or AAV-Cre-GFP (C). Arrows denote *Bdnf* mRNA signals in the PVH.

(D) Body weight of female $Bdnf^{lox/lox}$ mice injected with either AAV-GFP or AAV-Cre-GFP. Two-way ANOVA indicates a significant difference in body weight between the 2 groups: $F_{(1, 153)} = 124.56$, $P < 0.001$.

(E) Body weight of female $Bdnf^{lox/lox}$ mice injected with either AAV-GFP or AAV-Cre-GFP. Two-way ANOVA indicates a significant difference in body weight among the 3 groups: $F_{(2, 144)} = 116.81$, $P < 0.001$. ** $P < 0.01$ and *** $P < 0.001$ when compared to the AAV-GFP group using Bonferroni post-hoc test. $^{\#\#}$ $P < 0.01$ and $^{\#\#\#}$ $P < 0.001$ when the AAV-Cre-GFP (AMP) group was compared to the AAV-Cre-GFP (MP) group using Bonferroni post-hoc test.

(F) Daily food intake during the 4th week of the post-injection period. The numbers inside columns indicate animal numbers.

(G) Correlation between the extent of AAV infection in the anterior PVH and hyperphagia. The data used in the plot is from the animals listed in Figure S3G, except animal AAV-Cre-GFP2 in which AAV infection in the PVH was minimal. $P < 0.001$.

(H) Locomotor activity of $Bdnf^{lox/lox}$ mice 9 weeks after AAV injection. Animal number was 8, 5, and 6 for AAV-GFP, AAV-Cre-GFP (MP), and AAV-Cre-GFP (AMP), respectively.

Error bars indicate standard errors. See also Figure S3.

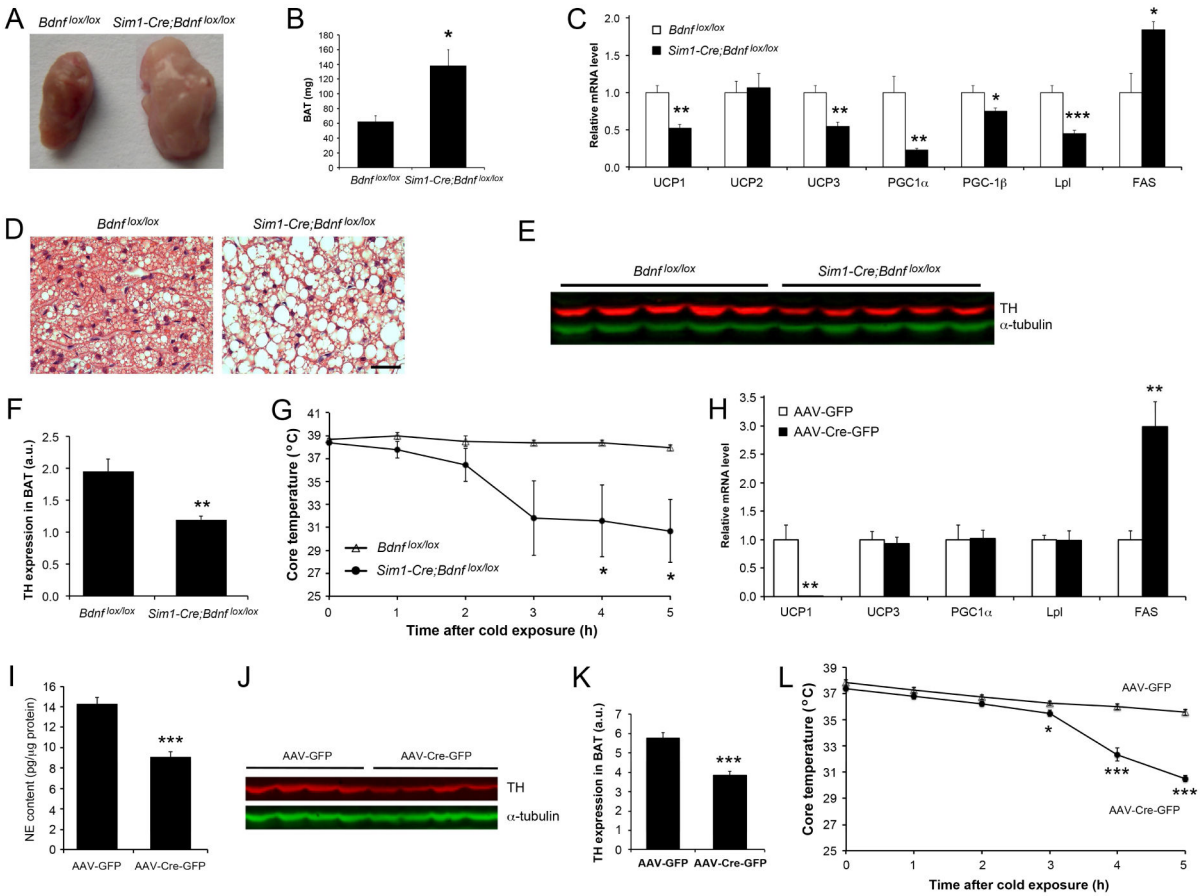


**Figure 5. Impaired adaptive thermogenesis in mice where *Bdnf* is deleted in the PVH**

(A and B) Appearance and mass of iBAT in *Bdnf*$^{lox/lox}$ and *Sim1-Cre;Bdnf*$^{lox/lox}$ mice at 8 weeks of age.

(C) Levels of mRNAs in iBAT of *Bdnf*$^{lox/lox}$ and *Sim1-Cre;Bdnf*$^{lox/lox}$ mice at 8 weeks of age (n=5 mice per genotype).

(D) H&E staining of iBAT sections from *Bdnf*$^{lox/lox}$ and *Sim1-Cre;Bdnf*$^{lox/lox}$ mice at 8 weeks of age. Scale bar, 50 μm.

(E) Immunoblotting of iBAT extracts from mice at 8 weeks of age using antibodies against tyrosine hydroxylase (TH) and α-tubulin.

(F) Quantification of the immunoblot described in (E).

(G) Rectal temperature of mice at 10 weeks of age after exposure to 10°C (n=5 mice per genotype).

(H) Levels of mRNAs in iBAT of *Bdnf*$^{lox/lox}$ mice injected with either AAV-Cre (n=5) or AAV-Cre-GFP (n=7).

(I) Levels of norepinephrine (NE) in iBAT of *Bdnf*$^{lox/lox}$ mice injected with either AAV-Cre (n=9) or AAV-Cre-GFP (n=15).

(J) Immunoblotting of iBAT extracts from *Bdnf*$^{lox/lox}$ mice injected with either AAV-Cre or AAV-Cre-GFP using antibodies against TH and α-tubulin.

(K) Quantification of the immunoblot described in (J).

(L) Rectal temperature of *Bdnf*$^{lox/lox}$ mice injected with either AAV-Cre (n=5) or AAV-Cre-GFP (n=5) after exposure to 10°C.

Error bars indicate standard errors. See also Figures S4.

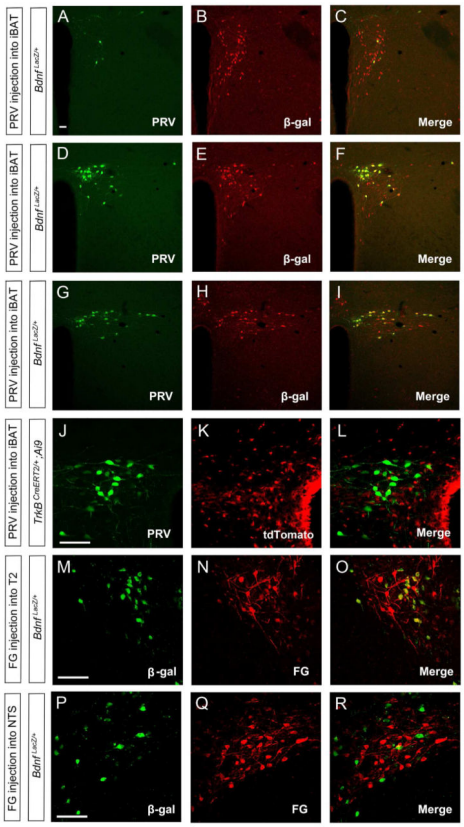


**Figure 6. Direct projection of BDNF neurons in the PVH to the spinal cord**

(A–I) Confocal images revealing that some BDNF neurons marked by β-galactosidase (β-gal) were labeled by PRV injected into iBAT in the anterior PVH (A–C), medial PVH (D–F), and posterior PVH (G–I).

(J–L) Representative confocal images showing that PVH neurons labeled by PRV injected into iBAT are distinct from TrkB neurons marked by tdTomato.

(M–O) Confocal images showing that fluorogold (FG) injected into T2 segment of the spinal cord labels many BDNF neurons in the PVH.

(P–R) Confocal images showing that fluorogold injected into the NTS labels only a small number of BDNF neurons in the PVH.

The scale bars represent 50 μm. See also Figures S5 and S6.

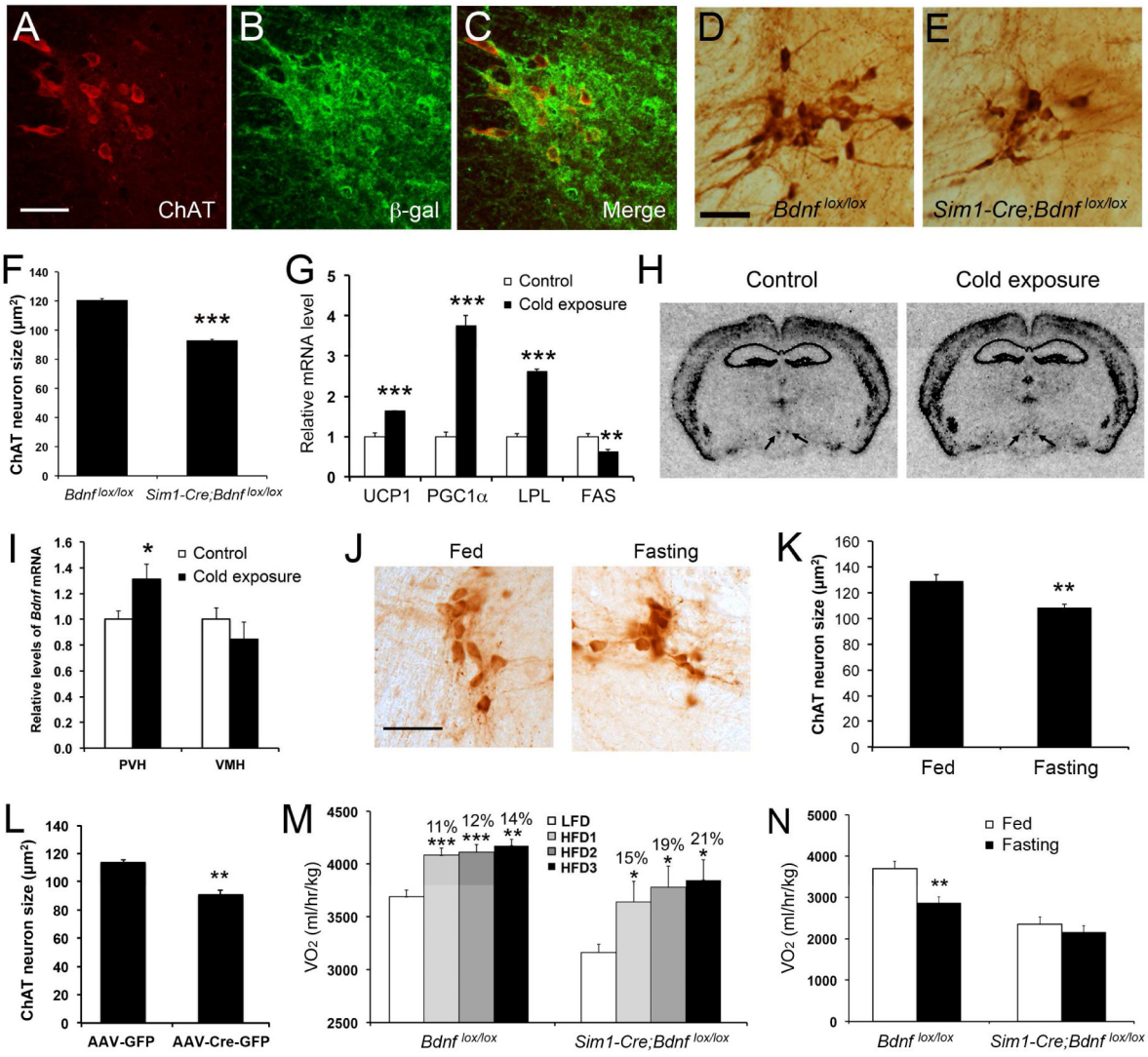


**Figure 7. The role of PVH BDNF in adaptive thermogenesis**

(A–C) Confocal images revealing coexpression of ChAT and β-galactosidase in the thoracic IML of *TrkB*$^{LacZ/+}$ mice.

(D–F) Atrophy of ChAT neurons in the thoracic IML of *Sim1-Cre;Bdnf*$^{lox/lox}$ mice (n=5 mice per genotype).

(G) Levels of mRNA for thermogenic genes in iBAT, analyzed with real-time PCR. C57BL/6J mice were housed at room temperature or 10°C for 3 days (n=4 mice per group).

(H) Representative images of in situ hybridization for *Bdnf* mRNA. C57BL/6J mice were housed at room temperature or 10°C for 3 days. Arrows denote the PVH.

(I) Quantification of *Bdnf* mRNA levels in the PVH and VMH of cold-exposed mice.

(J and K) Atrophy of ChAT neurons in the thoracic IML of food-deprived mice. C57BL/6J mice were deprived of food for 2 days (n=5 mice per group).

(L) Cell body size of ChAT neurons in the thoracic IML of *Bdnf*$^{lox/lox}$ mice injected with either AAV-GFP or AAV-Cre-GFP into the PVH (n=4 mice per group).

(M) Energy expenditure of *Bdnf*$^{lox/lox}$ and *Sim1-Cre;Bdnf*$^{lox/lox}$ mice during low-fat diet feeding (LFD) and subsequent 3-day HFD feeding (HFD1, HFD2 and HFD3). The numbers indicate % increase in $VO_2$ over the LFD control. Mouse number was 4 or 5 per genotype. (N) Energy expenditure of *Sim1-Cre;Bdnf*$^{lox/lox}$ mice during food deprivation (n=4–6 mice per genotype).

The scale bar represents 50 μm. Error bars indicate standard errors. See also Figure S7